EM mass splitting with infinite volume reconstruction

Luchang Jin

University of Connecticut

July 23, 2024

Isospin-Breaking Effects on Precision Observables in Lattice QCD

MITP - Mainz Institute for Theoretical Physics, Johannes Gutenberg University Mainz

Outline

- Introduction
- QED correction to light meson mass
- Operator renormalization via operator product expansion (OPE)
- QED correction to light meson leptonic decay width
- Summary

- QCD + QED is needed for sub-percent accuracy. Already very relevant at present.
- Possible approaches:
  - QCD + QED simulations: QED_L, massive photon, C^* boundary condition.
  - Perturbatively adding QED (RM123 approach): QED_L, massive photon, QED_∞.
- Our overall strategy (RM123 with QED_∞):
  - Calculate the pure QCD matrix elements of local vector currents.
  - Combine with analytical photon propagator in infinite volume.

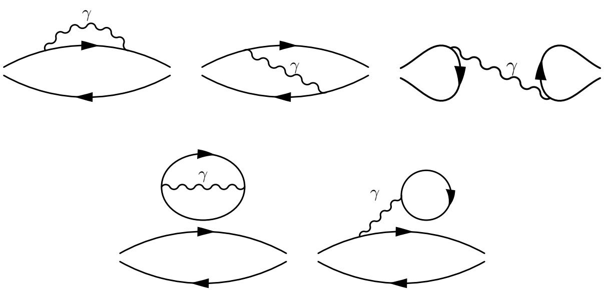

- One may analytically (and perturbatively) treat the QED part of the diagram in the **infinite volume** (and in the continuum) to eliminate the power-law suppressed finite volume effects due to the massless photons.
  - Hadronic vacuum polarization (HVP) contribution to muon $g-2$:

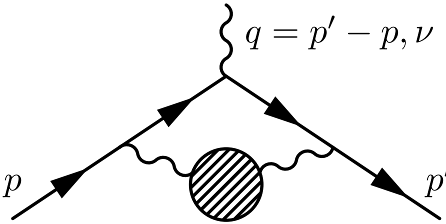

$$a_\mu^{\text{HVP LO}} = \left(\frac{\alpha}{\pi}\right)^2 \int_0^\infty dK^2 f(K^2) \hat{\Pi}(K^2) = \sum_{t=0}^{+\infty} w(t) C(t) \quad (1)$$

$$C(t) = \frac{1}{3} \sum_{\vec{x}} \sum_{j=0,1,2} \langle J_j^{em}(\vec{x}, t) J_j^{em}(0) \rangle_{\text{QCD}} \quad (2)$$

T. Blum (2003) D. Bernecker, H. Meyer (2011)

- One may analytically (and perturbatively) treat the QED part of the diagram in the **infinite volume** (and in the continuum) to eliminate the power-law suppressed finite volume effects due to the massless photons.
  - QED corrections to the hadronic vacuum polarization (HVP):

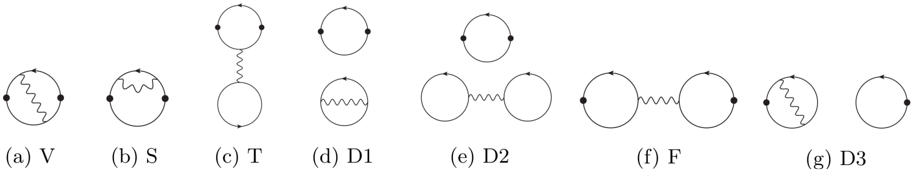

$$S^{\gamma}_{\mu,\nu}(x) = \frac{\delta_{\mu,\nu}}{4\pi^2 x^2} \tag{3}$$

T. Blum et al (2018)

Lattice QCD + QED_∞ and finite volume effects

- One may analytically (and perturbatively) treat the QED part of the diagram in the **infinite volume** (and in the continuum) to eliminate the power-law suppressed finite volume effects due to the massless photons.
  - Hadronic light-by-light (HLbL) contribution to muon $g-2$:

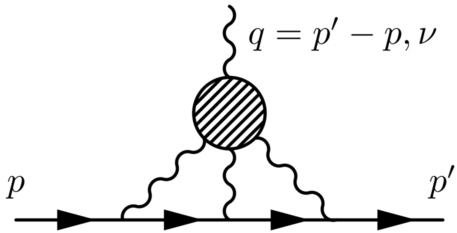

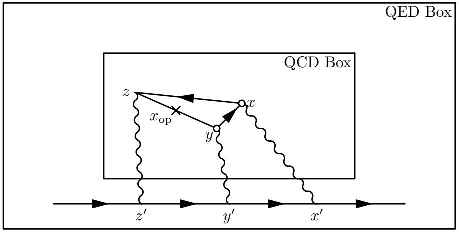

N. Asmussen et al (2016) T. Blum et al (2017)

- One may analytically (and perturbatively) treat the QED part of the diagram in the **infinite volume** (and in the continuum) to eliminate the power-law suppressed finite volume effects due to the massless photons.

- Does **NOT** work for calculating the QED correction to the mass of a stable hadron.

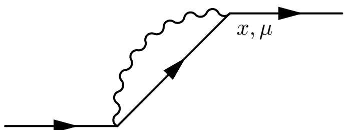

$$\Delta M = \mathcal{I} = \frac{1}{2}\int d^4x\, \mathcal{H}_{\mu,\nu}(x) S^{\gamma}_{\mu,\nu}(x), \quad (4)$$

$$\mathcal{H}_{\mu,\nu}(x) = \frac{1}{2M}\langle N|T J_\mu(x) J_\nu(0)|N\rangle, \quad S^{\gamma}_{\mu,\nu}(x) = \frac{\delta_{\mu,\nu}}{4\pi^2 x^2} \quad (5)$$

  – The hadronic function does not always fall exponentially in the long distance region. When $t \gg |\vec{x}|$:

$$\mathcal{H}_{\mu,\nu}(t,\vec{x}) \sim e^{-M\left(\sqrt{t^2+\vec{x}^2}-t\right)} \sim e^{-M\frac{\vec{x}^2}{2t}} \sim O(1) \quad (6)$$

  – Truncate the integral: $\int d^4x \to \int_{-L/2}^{L/2} d^4x$ & Approx the $\mathcal{H}(x)$: $\mathcal{H}(x) \to \mathcal{H}^L(x)$ $\to$ Power-law suppressed finite volume errors.

QED correction to hadron masses

$$\Delta M = \mathcal{I} = \frac{1}{2}\int d^4x \, \mathcal{H}_{\mu,\nu}(x) S^{\gamma}_{\mu,\nu}(x)$$

$$\mathcal{H}_{\mu,\nu}(x) = \frac{1}{2M}\langle N | T J_\mu(x) J_\nu(0) | N\rangle$$

$$S^{\gamma}_{\mu,\nu}(x) = \frac{\delta_{\mu,\nu}}{4\pi^2 x^2}$$

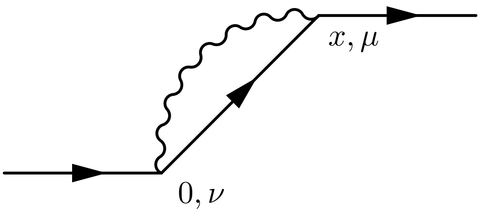

- Evaluate the QED part, the photon propagator, in infinite volume.
- The hadronic function does not always fall exponentially in the long distance region
  $\rightarrow$ Separate the integral into two parts ($t_s \lesssim L$):

$$\Delta M = \mathcal{I} = \mathcal{I}^{(s)} + \mathcal{I}^{(l)}$$

$$\mathcal{I}^{(s)} = \frac{1}{2}\int_{-t_s}^{t_s} dt \int d^3x \, \mathcal{H}_{\mu,\nu}(x) S^{\gamma}_{\mu,\nu}(x)$$

$$\mathcal{I}^{(l)} = \int_{t_s}^{\infty} dt \int d^3x \, \mathcal{H}_{\mu,\nu}(x) S^{\gamma}_{\mu,\nu}(x)$$

- For the short distance part, $\mathcal{I}^{(s)}$ can be directly calculated on a finite volume lattice:

$$\mathcal{I}^{(s)} \approx \mathcal{I}^{(s,L)} = \frac{1}{2}\int_{-t_s}^{t_s} dt \int_{L/2}^{L/2} d^3x \, \mathcal{H}^{L}_{\mu,\nu}(x) S^{\gamma}_{\mu,\nu}(x)$$

- For the **long distance part**, $\mathcal{I}^{(l)}$, a different treatment is required.

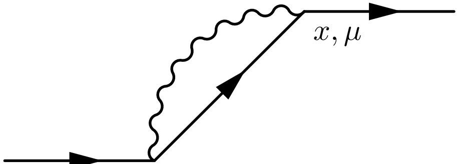

- For the long distance part, we can evaluate $\mathcal{H}_{\mu,\nu}(x)$ **indirectly** in the **infinite volume**.

$$\mathcal{I}^{(l)} = \int_{t_s}^{\infty} dt \int d^3x \, \mathcal{H}_{\mu,\nu}(x) S^{\gamma}_{\mu,\nu}(x)$$

- Note that when t is large ($t > t_s$), the intermediate states between the two currents are dominated by the single particle states (possibly with small momentum). Therefore:

$$\mathcal{H}_{\mu,\nu}(x) \approx \int \frac{d^3p}{(2\pi)^3} \left[\frac{1}{2E_{\vec{p}}} \frac{1}{2M} \langle N|J_\mu(0)|N(\vec{p})\rangle \langle N(\vec{p})|J_\nu(0)|N\rangle \right] e^{i\vec{p}\cdot\vec{x}-(E_{\vec{p}}-M)t}$$

  – We only need to calculate the form factors: $\langle N(\vec{p})|J_\nu(0)|N\rangle$!
  – Values for all $\vec{p}$ are needed. Inversely Fourier transform the above relation **at** t_s!

$$\int d^3x \, \mathcal{H}_{\mu,\nu}(t_s, \vec{x}) e^{-i\vec{p}\cdot\vec{x}+(E_{\vec{p}}-M)t_s} \approx \frac{1}{2E_{\vec{p}}} \frac{1}{2M} \langle N|J_\mu(0)|N(\vec{p})\rangle \langle N(\vec{p})|J_\nu(0)|N\rangle$$

- The final expression for QED correction to hadron mass is split into two parts:

$$\Delta M = \mathcal{I} = \mathcal{I}^{(s)} + \mathcal{I}^{(l)}$$

- For the short distance part: $\mathcal{I}^{(s)} \approx \mathcal{I}^{(s,L)} = \frac{1}{2}\int_{-t_s}^{t_s} dt \int_{L/2}^{L/2} d^3x\, \mathcal{H}^L_{\mu,\nu}(x) S^{\gamma}_{\mu,\nu}(x)$

- For the long distance part: $\mathcal{I}^{(l)} \approx \mathcal{I}^{(l,L)} = \int_{-L/2}^{L/2} d^3x\, \mathcal{H}^L_{\mu,\nu}(t_s,\vec{x}) L_{\mu,\nu}(t_s,\vec{x})$

- For Feynman gauge:

$$S^{\gamma}_{\mu,\nu}(x) = \frac{\delta_{\mu,\nu}}{4\pi^2 x^2} \qquad L_{\mu,\nu}(t_s,\vec{x}) = \frac{\delta_{\mu,\nu}}{2\pi^2}\int_0^{\infty} dp \frac{\sin(p|\vec{x}|)}{2(p+E_p-M)|\vec{x}|} e^{-pt_s}$$

- Only use $\mathcal{H}^L_{\mu,\nu}(t,\vec{x})$ within $-t_s \le t \le t_s$.

- Choose $t_s = L/2$, **finite volume errors and the ignored excited states contribution to $\mathcal{I}^{(l)}$ are both exponentially suppressed by the spatial lattice size L.**

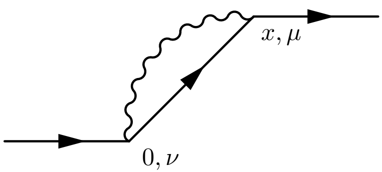

X. Feng, L. Jin. PRD [arXiv:1812.09817]

N. H. Christ, et al. PRD [arXiv:2304.08026]

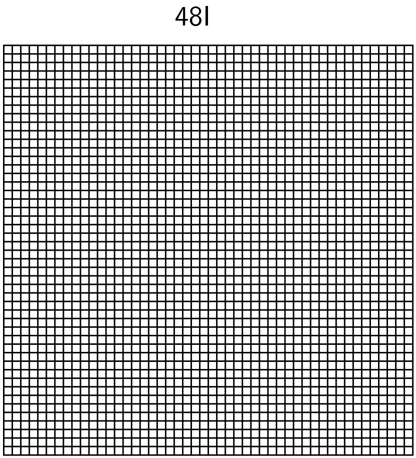

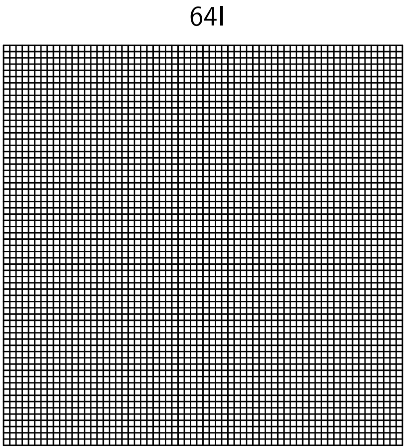

- Domain wall fermion action (preserves Chiral symmetry, no $\mathcal{O}(a)$ lattice artifacts).
- Iwasaki gauge action.
- $M_\pi = 139$ MeV, $L = 5.5$ fm box, $1/a_{48\text{I}} = 1.73$ GeV, $1/a_{64\text{I}} = 2.359$ GeV.

RBC/UKQCD, PRD [arXiv:1411.7017]

Hadronic matrix elements - meson mass

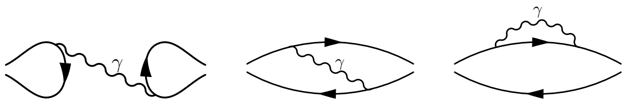

π^0 $\qquad$ π, K $\qquad$ π, K

$$H^{(s)}_{\rho,\sigma}(x_t, \vec{x}) = H^{(s)}_{\rho,\sigma}(x) = \frac{1}{2m_\pi}\langle \pi(\vec{0})|T\{J^{\mathrm{EM}}_\rho(x) J^{\mathrm{EM}}_\sigma(0)\}|\pi(\vec{0})\rangle \tag{7}$$

- Calculated with the 48I ensemble.
- Coulomb gauge fixed wall sources propagator at all time slices and point source propagators at randomly selected 2048 locations. We save these propagators after sparsening (1/16 ratio).
- Wall sources to interpolate the meson state.
- Keep the time separation between the wall sources and its closest J^{EM} operator fixed at a large enough distance (~ 1.5 fm) to control the excited state effects.
- Use point sources at one J^{EM} location, perform contraction at the other J^{EM} location after sparsening.

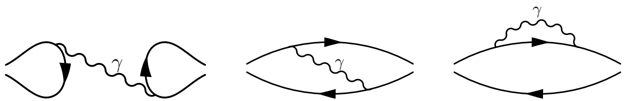

π^0 π, K π, K

$$H^{(s)}_{\rho,\sigma}(x_t, \vec{x}) = H^{(s)}_{\rho,\sigma}(x) = \frac{1}{2m_\pi}\langle \pi(\vec{0})|T\{J^{\mathrm{EM}}_\rho(x)J^{\mathrm{EM}}_\sigma(0)\}|\pi(\vec{0})\rangle \tag{8}$$

$$H^{(s)}_{\mu\mu}(t, r) = \int d^3\vec{x}\,\delta(|\vec{x}| - r)H^{(s)}_{\mu,\mu}(t, \vec{x}) \to \sum_{\vec{x},|\vec{x}|=r} H^{(s)}_{\mu,\mu}(t, \vec{x}) \tag{9}$$

$$\frac{1}{4\pi|\vec{x}|^2}H^{(s)}_{\mu\mu}(t, r) = \frac{\int d^3\vec{x}\,\delta(|\vec{x}| - r)H^{(s)}_{\mu\mu}(t, \vec{x})}{\int d^3\vec{x}\,\delta(|\vec{x}| - r)} \tag{10}$$

$$\to \frac{\sum_{\vec{x},|\vec{x}|=r} H^{(s)}_{\mu,\mu}(t, \vec{x})}{\sum_{\vec{x},|\vec{x}|=r} 1} \tag{11}$$

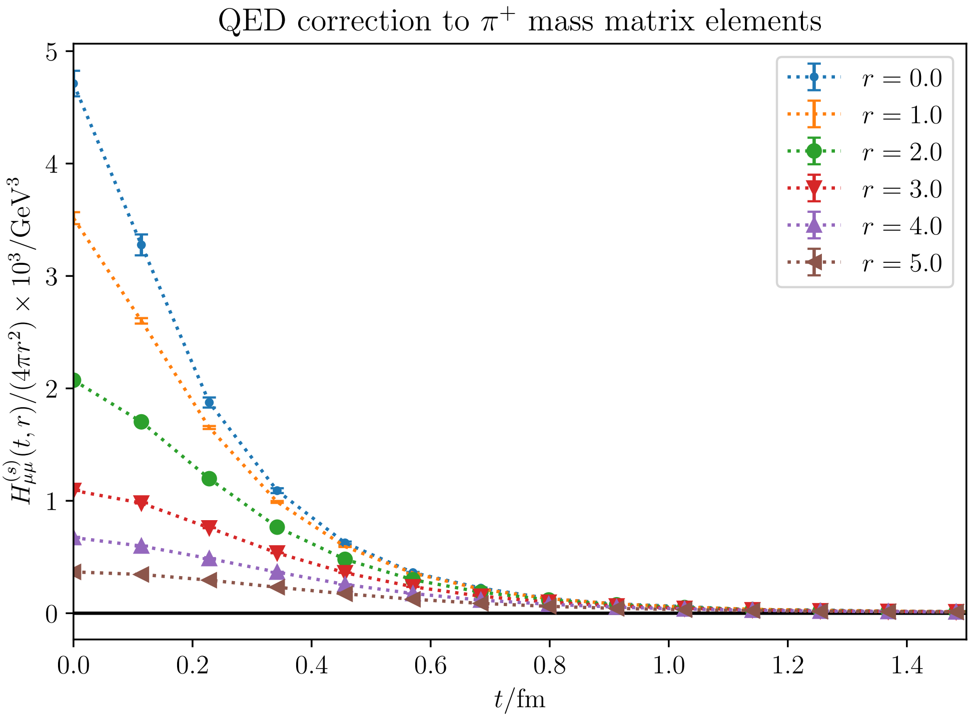
QED correction to π^+ mass matrix elements
$H^{(s)}_{\mu\mu}(t,r)/(4\pi r^2) \times 10^3/\mathrm{GeV}^3$
t/fm
$r = 0.0$
$r = 1.0$
$r = 2.0$
$r = 3.0$
$r = 4.0$
$r = 5.0$
0
1
2
3
4
5
0.0
0.2
0.4
0.6
0.8
1.0
1.2
1.4

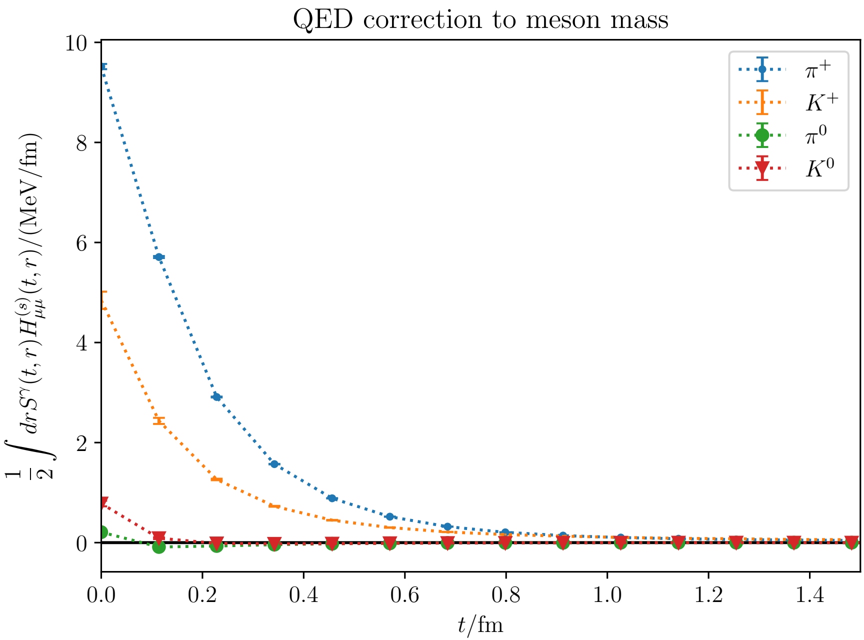

- Integrate over t (from $-\infty$ to $+\infty$) give the meson mass shift.

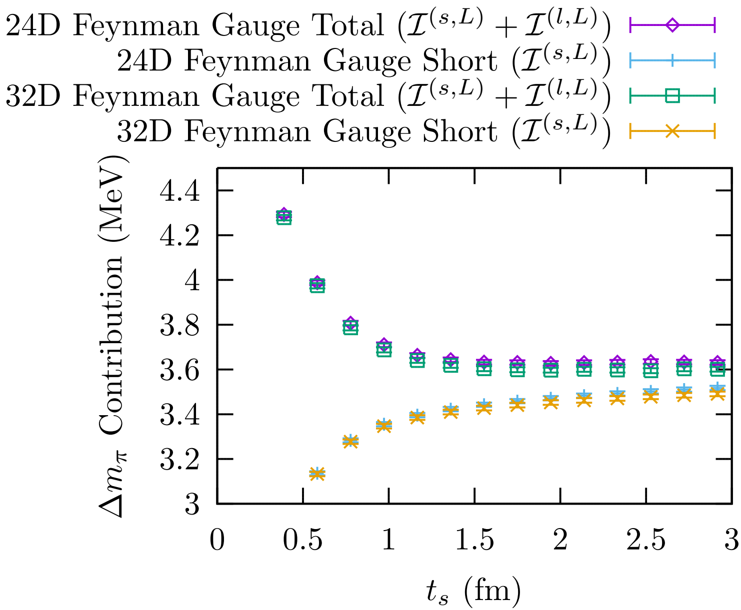

- The difference between 32D and 24D is $-0.035(16)$MeV. This is consistent with a scalar QED calculation, which yields -0.022MeV.

X. Feng, et al, PRL [arXiv:2108.05311]

Continuum extrapolation of Δm_π

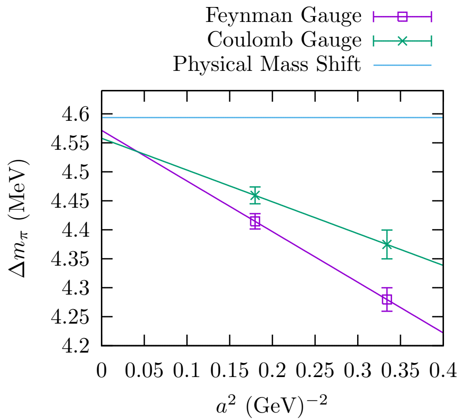

	Disc (MeV)	Conn (MeV)	Total (MeV)
Feyn	0.051(9)(22)	4.483(40)(28)	4.534(42)(43)
Coul	0.052(2)(13)	4.508(46)(42)	4.560(46)(41)
Coul-t	0.018(1)(4)	1.840(22)(39)	1.858(22)(41)

Finite volume corrections (the differences between the 32D and 24D ensembles) are included in table.

X. Feng, et al, PRL [arXiv:2108.05311]

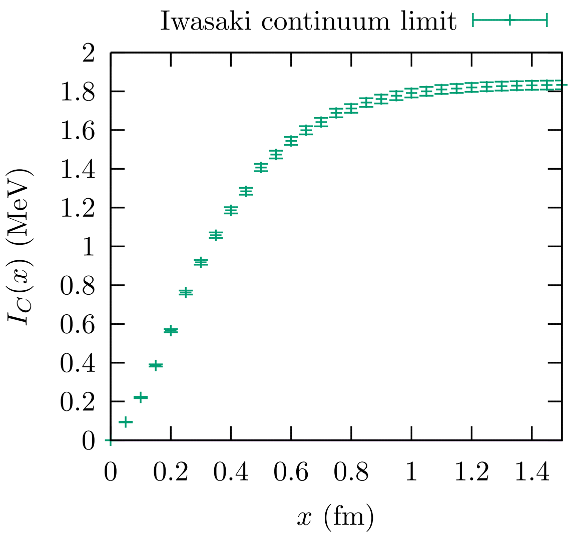

- The Coulomb potential contribution to the pion mass difference. The curve is the partial sum respect to the spatial separation of the two equal-time current operators.
- This plot provide some interesting pion shape information.

X. Feng, et al, PRL [arXiv:2108.05311]

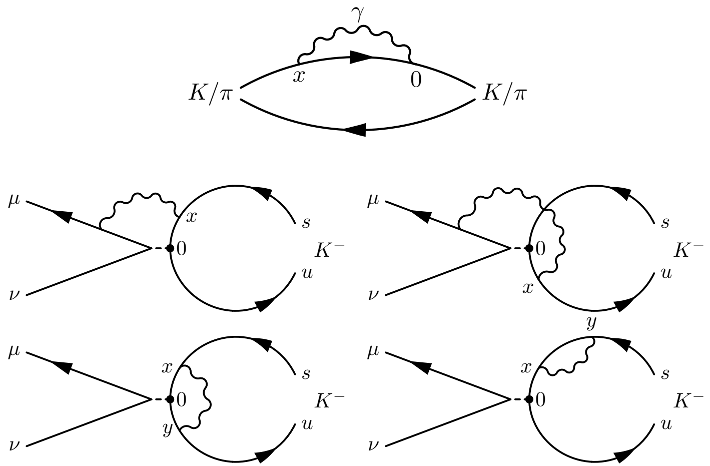

- Logarithmic divergences will arise in the integral when x (and y) is close to 0.
- Need renormalization to accomodate these divergences, and match lattice results to $\overline{\text{MS}}$ results.
- The short distance behaviour can be obtained via operator product expansion (OPE).

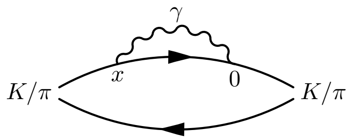

- Consider the self-energy diagram. Logarithmic divergences will arise in the integral when x is close to 0. Use OPE relation:

$$\text{AVG } x \text{ DIR } \left\{ T J_\mu^s(\frac{x}{2}) J_\mu^s(-\frac{x}{2}) \right\} = C_m(x^2) m_s \bar{s}(0) s(0) + \cdots \quad (12)$$

where $J_\mu^s(x) = \bar{s}(x)\gamma_\mu s(x)$, relation $\rightarrow$ implies after average over x directions.

$$C_m(x^2) = \frac{3}{2\pi^2 x^2} \quad (13)$$

at tree level [M. A. Shifman et al, Nucl.Phys.B 147 (1979) 385-447].

- Renormalization strategy for m_s is to match the following matrix elements:

$$H^{K,s}(\Lambda) = \langle K^+ | m_s \bar{s}(0) s(0) + e_s^2 \int_{|x|<1/\Lambda} d^4x \, S^\gamma(x^2) T J_\mu^s(\frac{x}{2}) J_\mu^s(-\frac{x}{2}) | K^+ \rangle \quad (14)$$

between lattice and $\overline{\text{MS}}$.

Operator renormalization via OPE

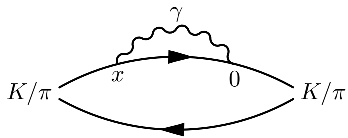

- Renormalization strategy for m_s is to match the following matrix elements:

$$H^{K,s}(\Lambda) = \langle K^+ | m_s \bar{s}(0) s(0) + e_s^2 \int_{|x|<1/\Lambda} d^4x \, S^\gamma(x^2) T J_\mu^s(\frac{x}{2}) J_\mu^s(-\frac{x}{2}) | K^+ \rangle \tag{15}$$

between lattice and $\overline{\text{MS}}$.

- For $\overline{\text{MS}}$

$$H^{K,s}(\Lambda) \approx m_s^{\overline{\text{MS}}} \left(1 + e_s^2 \int_{|x|<1/\Lambda} d^4x \, S^\gamma(x^2) C_m(x^2) \right) \langle K^+ | \bar{s}(0) s(0) | K^+ \rangle^{\overline{\text{MS}}} \tag{16}$$

- For lattice

$$H^{K,s}(\Lambda) \approx m_s^{\text{latt}} \left(1 + e_s^2 \sum_{|x|<1/\Lambda} S^{\gamma,\text{latt}}(x^2) \frac{\langle K^+ | T J_\mu^s(\frac{x}{2}) J_\mu^s(-\frac{x}{2}) | K^+ \rangle^{\text{latt}}}{m_s^{\text{latt}} \langle K^+ | \bar{s}(0) s(0) | K^+ \rangle^{\text{latt}}} \right) \langle K^+ | \bar{s}(0) s(0) | K^+ \rangle^{\text{latt}} \tag{17}$$

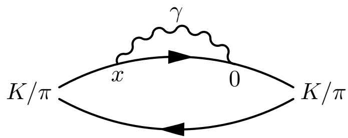

- For $\overline{\text{MS}}$

$$H^{K,s}(\Lambda) \approx m_s^{\overline{\text{MS}}}\left(1 + e_s^2 \int_{|x|<1/\Lambda} d^4x\, S^\gamma(x^2) C_m(x^2)\right) \langle K^+|\bar{s}(0)s(0)|K^+\rangle^{\overline{\text{MS}}} \tag{18}$$

- For lattice

$$H^{K,s}(\Lambda) \approx m_s^{\text{latt}}\left(1 + e_s^2 \sum_{|x|<1/\Lambda} S^{\gamma,\text{latt}}(x^2) \frac{\langle K^+|T J_\mu^s(\frac{x}{2}) J_\mu^s(-\frac{x}{2})|K^+\rangle^{\text{latt}}}{m_s^{\text{latt}}\langle K^+|\bar{s}(0)s(0)|K^+\rangle^{\text{latt}}}\right) \langle K^+|\bar{s}(0)s(0)|K^+\rangle^{\text{latt}} \tag{19}$$

- Define Z_S^{QCD} via $Z_S^{\text{QCD}}\langle K^+|\bar{s}(0)s(0)|K^+\rangle^{\text{latt}} = \langle K^+|\bar{s}(0)s(0)|K^+\rangle^{\overline{\text{MS}}}$ and obtain:

$$\begin{aligned} m_s^{\overline{\text{MS}}} = & \frac{1}{Z_S^{\text{QCD}}} m_s^{\text{latt}}\Bigg(1 - e_s^2 \int_{|x|<1/\Lambda} d^4x\, S^\gamma(x^2) C_m(x^2) \\ & + e_s^2 \sum_{|x|<1/\Lambda} S^{\gamma,\text{latt}}(x^2) \frac{\langle K^+|T J_\mu^s(\frac{x}{2}) J_\mu^s(-\frac{x}{2})|K^+\rangle^{\text{latt}}}{m_s^{\text{latt}}\langle K^+|\bar{s}(0)s(0)|K^+\rangle^{\text{latt}}}\Bigg) \end{aligned} \tag{20}$$

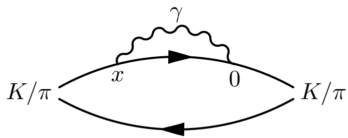

- Define Z_S^{QCD} via $Z_S^{\text{QCD}}\langle K^+|\bar{s}(0)s(0)|K^+\rangle^{\text{latt}} = \langle K^+|\bar{s}(0)s(0)|K^+\rangle^{\overline{\text{MS}}}$ and obtain:

$$m_s^{\overline{\text{MS}}} = \frac{1}{Z_S^{\text{QCD}}} m_s^{\text{latt}} \Bigg(1 - e_s^2 \int_{|x|<1/\Lambda} d^4x\, S^{\gamma}(x^2) C_m(x^2) + e_s^2 \sum_{|x|<1/\Lambda} S^{\gamma,\text{latt}}(x^2) \frac{\langle K^+|T J_\mu^s(\frac{x}{2}) J_\mu^s(-\frac{x}{2})|K^+\rangle^{\text{latt}}}{m_s^{\text{latt}}\langle K^+|\bar{s}(0)s(0)|K^+\rangle^{\text{latt}}} \Bigg) \tag{21}$$

- Require a window $|x| \sim 1/\Lambda$ where:

$$m_s^{\text{latt}} C_m(x^2) \approx \text{AVG } x \text{ DIR} \left\{ \frac{\langle K^+|T J_\mu^s(\frac{x}{2}) J_\mu^s(-\frac{x}{2})|K^+\rangle^{\text{latt}}}{\langle K^+|\bar{s}(0)s(0)|K^+\rangle^{\text{latt}}} \right\} \tag{22}$$

- Similarly:

$$m_d^{\text{latt}} C_m(x^2) \approx \text{AVG } x \text{ DIR} \left\{ \frac{\langle \pi^+|T J_\mu^d(\frac{x}{2}) J_\mu^d(-\frac{x}{2})|\pi^+\rangle^{\text{latt}}}{\langle \pi^+|\bar{d}(0)d(0)|\pi^+\rangle^{\text{latt}}} \right\} \tag{23}$$

Operator renormalization via OPE (prelim)

$$\frac{\text{AVG } x \text{ DIR} \left\{ \frac{\langle \pi^+ | T J^d_\mu(\frac{x}{2}) J^d_\mu(-\frac{x}{2}) | \pi^+ \rangle^{\text{latt}}}{\langle \pi^+ | \bar{d}(0) d(0) | \pi^+ \rangle^{\text{latt}}} \right\}}{m_d^{\text{latt}} C_m(x^2)} \quad \frac{\text{AVG } x \text{ DIR} \left\{ \frac{\langle K^+ | T J^s_\mu(\frac{x}{2}) J^s_\mu(-\frac{x}{2}) | K^+ \rangle^{\text{latt}}}{\langle K^+ | \bar{s}(0) s(0) | K^+ \rangle^{\text{latt}}} \right\}}{m_s^{\text{latt}} C_m(x^2)} \quad (24)$$

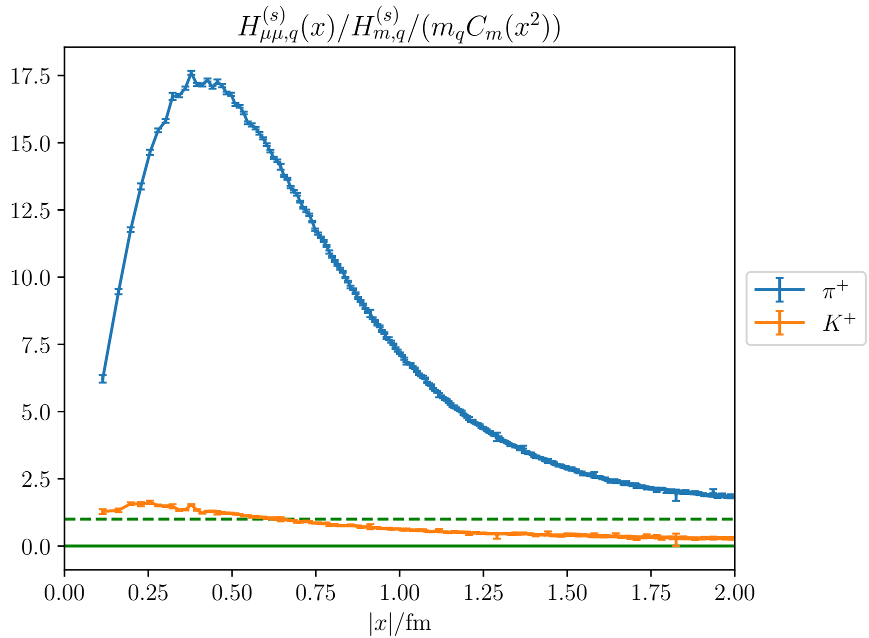

$$\frac{\text{AVG } x \text{ DIR}\left\{\frac{\langle K^+|TJ^s_\mu(\frac{x}{2})J^s_\mu(-\frac{x}{2})|K^+\rangle^{\text{latt}}}{\langle K^+|\bar{s}(0)s(0)|K^+\rangle^{\text{latt}}}\right\} - \text{AVG } x \text{ DIR}\left\{\frac{\langle \pi^+|TJ^d_\mu(\frac{x}{2})J^d_\mu(-\frac{x}{2})|\pi^+\rangle^{\text{latt}}}{\langle \pi^+|\bar{d}(0)d(0)|\pi^+\rangle^{\text{latt}}}\right\}}{m_s^{\text{latt}}C_m(x^2) - m_d^{\text{latt}}C_m(x^2)} \quad (25)$$

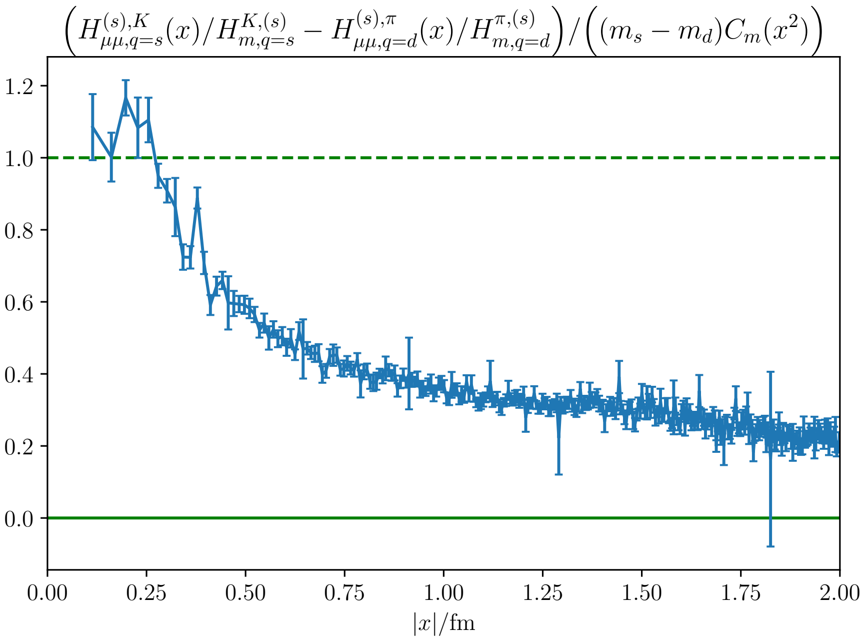

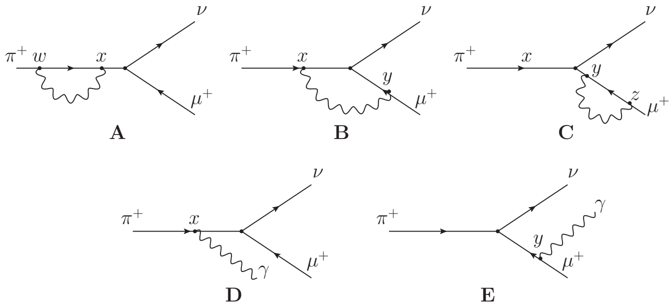

- χPT: V. Cirigliano and H. Neufeld. PLB [arXiv:1102.0563]

$$\delta R_K = 0.0064(24) \tag{26}$$

$$\delta R_\pi = 0.0176(21) \tag{27}$$

$$\delta R_{K\pi} = \delta R_K - \delta R_\pi = -0.0112(21) \tag{28}$$

- Lattice ETMC: M. Di Carlo, et al. PRD [arXiv:1904.08731]

$$\delta R_K = 0.0024(10) \tag{29}$$

$$\delta R_\pi = 0.0153(19) \tag{30}$$

$$\delta R_{K\pi} = \delta R_K - \delta R_\pi = -0.0126(14) \tag{31}$$

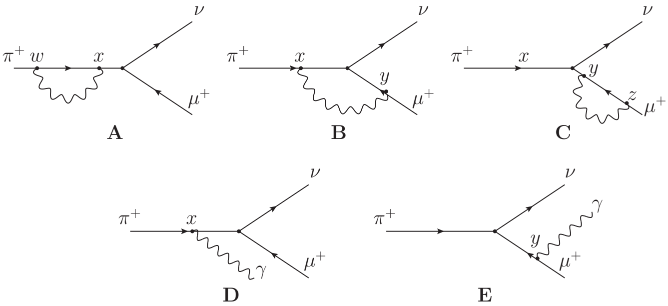

- Lattice ETMC: M. Di Carlo, et al. PRD [arXiv:1904.08731]

$$\delta R_K = 0.0024(10) \tag{32}$$

$$\delta R_\pi = 0.0153(19) \tag{33}$$

$$\delta R_{K\pi} = \delta R_K - \delta R_\pi = -0.0126(14) \tag{34}$$

- Lattice RBC-UKQCD: P. Boyle, et al. JHEP [arXiv:2211.12865]

$$\delta R_{K\pi} = -0.0086(3)_{\text{stat}}\left(\begin{smallmatrix}+11\\-4\end{smallmatrix}\right)_{\text{fit}}(5)_{\text{disc.}}(5)_{\text{quench.}}(39)_{\text{vol.}} \tag{35}$$

Also use 48I ensemble (physical pion mass). Major systematic error from finite volume effects.

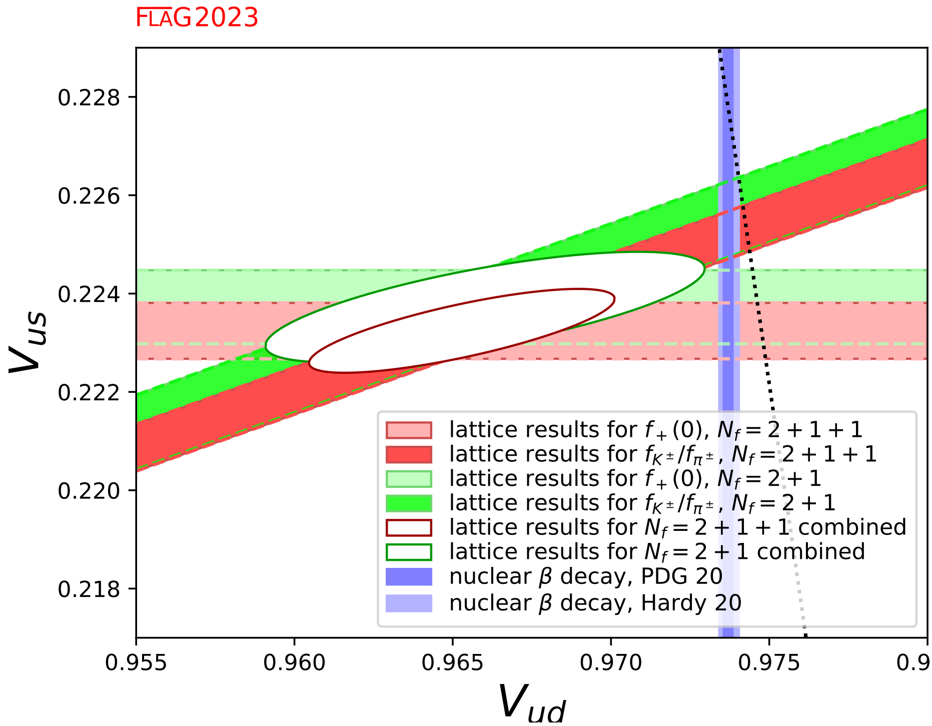
FLAG 2023
0.228
0.226
0.224
0.222
0.220
0.218
V_{us}
0.955
0.960
0.965
0.970
0.975
0.980
V_{ud}
lattice results for $f_+(0)$, $N_f = 2+1+1$
lattice results for $f_{K^\pm}/f_{\pi^\pm}$, $N_f = 2+1+1$
lattice results for $f_+(0)$, $N_f = 2+1$
lattice results for $f_{K^\pm}/f_{\pi^\pm}$, $N_f = 2+1$
lattice results for $N_f = 2+1+1$ combined
lattice results for $N_f = 2+1$ combined
nuclear β decay, PDG 20
nuclear β decay, Hardy 20

Hadronic matrix elements - leptonic decay

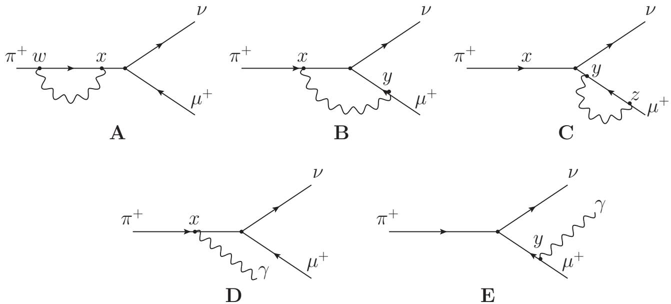

$$H_{\mu}^{(0)} = \langle 0 | J_{\mu}^{W}(0) | \pi(\vec{0}) \rangle \quad (36)$$

$$H_{\mu,\rho}^{(1)}(x) = H_{\mu,\rho}^{(1)}(x_t, \vec{x}) = \langle 0 | T\{ J_{\mu}^{W}(0) J_{\rho}^{\mathrm{EM}}(x) \} | \pi(\vec{0}) \rangle \quad (37)$$

$$H_{\mu,\rho,\sigma}^{(2)}(t_1, t_2, \vec{x}) = \int d^3\vec{w} \langle 0 | T\{ J_{\mu}^{W}(0) J_{\rho}^{\mathrm{EM}}(t_1, \vec{w} + \vec{x}) J_{\sigma}^{\mathrm{EM}}(t_2, \vec{w}) \} | \pi(\vec{0}) \rangle \quad (38)$$

- Calculated with the 48I ensemble.
- Coulomb gauge fixed wall sources propagator at all time slices and point source propagators at randomly selected 2048 locations. We save these propagators after sparsening (1/16 ratio).
- This is the same set of propagators as the meson mass calculation.

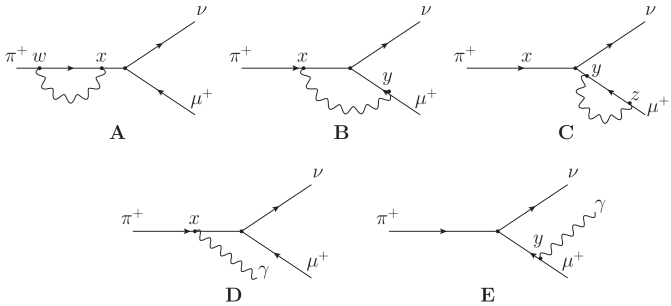

$$H_{\mu}^{(0)} = \langle 0 | J_{\mu}^{W}(0) | \pi(\vec{0}) \rangle \tag{39}$$

$$H_{\mu,\rho}^{(1)}(x) = H_{\mu,\rho}^{(1)}(x_t, \vec{x}) = \langle 0 | T\{J_{\mu}^{W}(0) J_{\rho}^{\mathrm{EM}}(x)\} | \pi(\vec{0}) \rangle \tag{40}$$

$$H_{\mu,\rho,\sigma}^{(2)}(t_1, t_2, \vec{x}) = \int d^3\vec{w} \langle 0 | T\{J_{\mu}^{W}(0) J_{\rho}^{\mathrm{EM}}(t_1, \vec{w}+\vec{x}) J_{\sigma}^{\mathrm{EM}}(t_2, \vec{w})\} | \pi(\vec{0}) \rangle \tag{41}$$

- Wall sources to interpolate the meson state.
- Keep the time separation between the wall sources and its closest J^{EM} or J^{W} operator fixed at a large enough distance (~ 1.5 fm) to control the excited state effects.
- $J_{\mu}^{W} = J_{\mu}^{W,V} - J_{\mu}^{W,A} = \bar{d}\gamma_{\mu}u + \bar{s}\gamma_{\mu}u - \bar{d}\gamma_{\mu}\gamma_5 u - \bar{s}\gamma_{\mu}\gamma_5 u.$

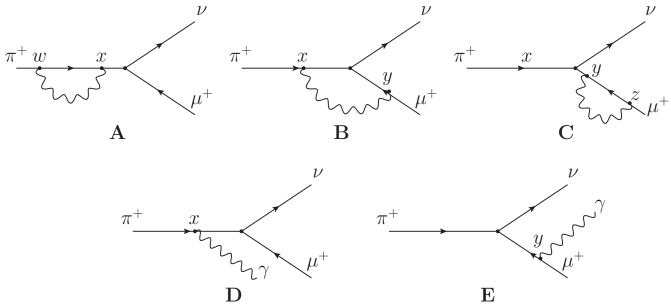

$$H_\mu^{(0)} = \langle 0 | J_\mu^W(0) | \pi(\vec{0}) \rangle \tag{42}$$

$$H_{\mu,\rho}^{(1)}(x) = H_{\mu,\rho}^{(1)}(x_t, \vec{x}) = \langle 0 | T\{J_\mu^W(0) J_\rho^{\mathrm{EM}}(x)\} | \pi(\vec{0}) \rangle \tag{43}$$

$$H_{\mu,\rho,\sigma}^{(2)}(t_1, t_2, \vec{x}) = \int d^3\vec{w} \langle 0 | T\{J_\mu^W(0) J_\rho^{\mathrm{EM}}(t_1, \vec{w}+\vec{x}) J_\sigma^{\mathrm{EM}}(t_2, \vec{w})\} | \pi(\vec{0}) \rangle \tag{44}$$

- For diagram B and D, use point sources at one J^{EM} location, perform contraction at the other J^{EM} location after sparsening.
- For diagram A, use point sources at one J^{EM} location and the J^W location, perform contract at the other J^{EM} location. Use aggresive sparsening to reduce the contraction cost.

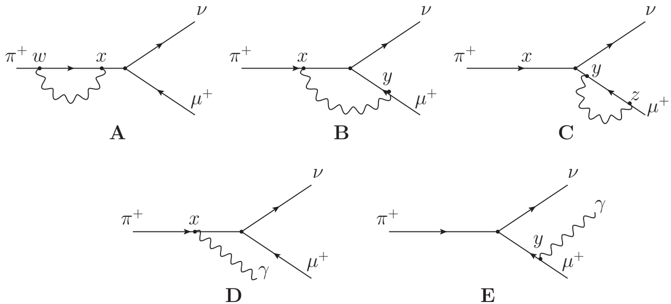

$$H^{(0)}_{\mu} = \langle 0|J^W_\mu(0)|\pi(\vec{0})\rangle \tag{45}$$

$$H^{(1)}_{\mu,\rho}(x) = H^{(1)}_{\mu,\rho}(x_t,\vec{x}) = \langle 0|T\{J^W_\mu(0)J^{EM}_\rho(x)\}|\pi(\vec{0})\rangle \tag{46}$$

$$H^{(2)}_{\mu,\rho,\sigma}(t_1,t_2,\vec{x}) = \int d^3\vec{w}\langle 0|T\{J^W_\mu(0)J^{EM}_\rho(t_1,\vec{w}+\vec{x})J^{EM}_\sigma(t_2,\vec{w})\}|\pi(\vec{0})\rangle \tag{47}$$

- For $H^{(0)}$:

$$H^{(0)}_{\mu} = -\delta_{\mu,t}\langle 0|J^{W,A}_t(0)|\pi(\vec{0})\rangle = -\delta_{\mu,t}\, i m_\pi f_\pi \tag{48}$$

where $f_\pi \approx 130$ MeV

Hadronic matrix elements - leptonic decay

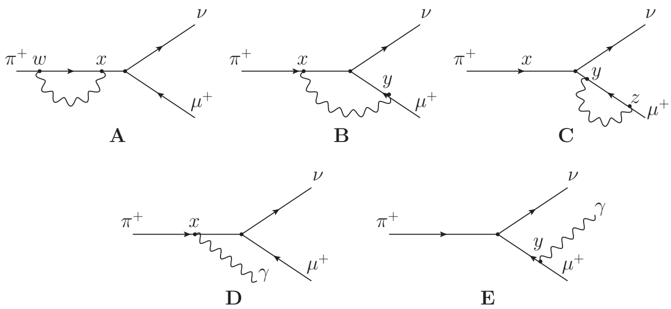

$$H^{(0)}_{\mu} = \langle 0 | J^{W}_{\mu}(0) | \pi(\vec{0}) \rangle \tag{49}$$

$$H^{(1)}_{\mu,\rho}(x) = H^{(1)}_{\mu,\rho}(x_t, \vec{x}) = \langle 0 | T\{J^{W}_{\mu}(0) J^{\mathrm{EM}}_{\rho}(x)\} | \pi(\vec{0}) \rangle \tag{50}$$

$$H^{(2)}_{\mu,\rho,\sigma}(t_1, t_2, \vec{x}) = \int d^3\vec{w} \langle 0 | T\{J^{W}_{\mu}(0) J^{\mathrm{EM}}_{\rho}(t_1, \vec{w}+\vec{x}) J^{\mathrm{EM}}_{\sigma}(t_2, \vec{w})\} | \pi(\vec{0}) \rangle \tag{51}$$

- For $H^{(2)}$:

$$H^{(2)}_{\mu,\rho,\sigma}(t_1, t_2, \vec{x}) = -\delta_{\mu,t} \int d^3\vec{w} \langle 0 | T\{J^{W,A}_{t}(0) J^{\mathrm{EM}}_{\rho}(t_1, \vec{w}+\vec{x}) J^{\mathrm{EM}}_{\sigma}(t_2, \vec{w})\} | \pi(\vec{0}) \rangle \tag{52}$$

$$H^{(2)}_{t\mu\mu}(t_1, t_2, r) = \int d^3\vec{x}\, \delta(|\vec{x}| - r) H^{(2)}_{t,\mu,\mu}(t_1, t_2, \vec{x}) \tag{53}$$

$$H^{(0)}_{\mu} = \langle 0|J^{W}_{\mu}(0)|\pi(\vec{0})\rangle \tag{54}$$

$$H^{(1)}_{\mu,\rho}(x) = H^{(1)}_{\mu,\rho}(x_t,\vec{x}) = \langle 0|T\{J^{W}_{\mu}(0)J^{\text{EM}}_{\rho}(x)\}|\pi(\vec{0})\rangle \tag{55}$$

$$H^{(2)}_{\mu,\rho,\sigma}(t_1,t_2,\vec{x}) = \int d^3\vec{w}\langle 0|T\{J^{W}_{\mu}(0)J^{\text{EM}}_{\rho}(t_1,\vec{w}+\vec{x})J^{\text{EM}}_{\sigma}(t_2,\vec{w})\}|\pi(\vec{0})\rangle \tag{56}$$

- For $H^{(1)}$:

$$H^{(1,V)}_{\mu,\rho}(x) = \langle 0|T\{J^{W,V}_{\mu}(0)J^{\text{EM}}_{\rho}(x)\}|\pi(\vec{0})\rangle \tag{57}$$

$$H^{(1,A)}_{\mu,\rho}(x) = \langle 0|T\{J^{W,A}_{\mu}(0)J^{\text{EM}}_{\rho}(x)\}|\pi(\vec{0})\rangle \tag{58}$$

$$H^{(1)}_{V}(t,r) = \frac{1}{2}\int d^3\vec{x}\,\delta(|\vec{x}|-r)\epsilon_{i,j,k}\,\frac{x_i}{|\vec{x}|}H^{(1,V)}_{j,k}(t,\vec{x}) \tag{59}$$

$$H^{(1)}_{Att}(t,r) = \int d^3\vec{x}\,\delta(|\vec{x}|-r)H^{(1,A)}_{t,t}(t,\vec{x}) \tag{60}$$

$$H^{(1)}_{Atx}(t,r) = \int d^3\vec{x}\,\delta(|\vec{x}|-r)\frac{x_i}{|\vec{x}|}H^{(1,A)}_{t,i}(t,\vec{x}) \tag{61}$$

$$H^{(1)}_{Axt}(t,r) = \int d^3\vec{x}\,\delta(|\vec{x}|-r)\frac{x_i}{|\vec{x}|}H^{(1,A)}_{i,t}(t,\vec{x}) \tag{62}$$

$$H^{(1)}_{Aii}(t,r) = \int d^3\vec{x}\,\delta(|\vec{x}|-r)\frac{1}{3}H^{(1,A)}_{i,i}(t,\vec{x}) \tag{63}$$

$$H^{(1)}_{Axx}(t,r) = \int d^3\vec{x}\,\delta(|\vec{x}|-r)\frac{3}{2}\left(\frac{x_i x_j}{|\vec{x}|^2}-\frac{1}{3}\delta_{i,j}\right)H^{(1,A)}_{i,j}(t,\vec{x}) \tag{64}$$

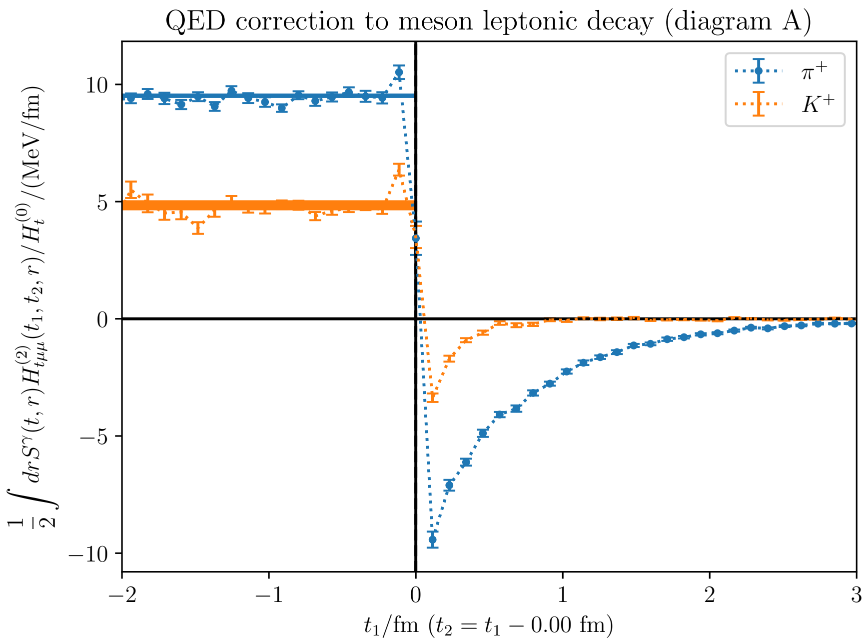

- Horizontal band represent the corresponding value from the mass shift calculation.

$$H^{(2)}_{t\mu\mu}(t_1, t_2, r)/H^{(0)}_t \approx H^{(s)}_{\mu\mu}(t_1 - t_2, r) \qquad (t_1, t_2 \ll 0) \qquad (65)$$

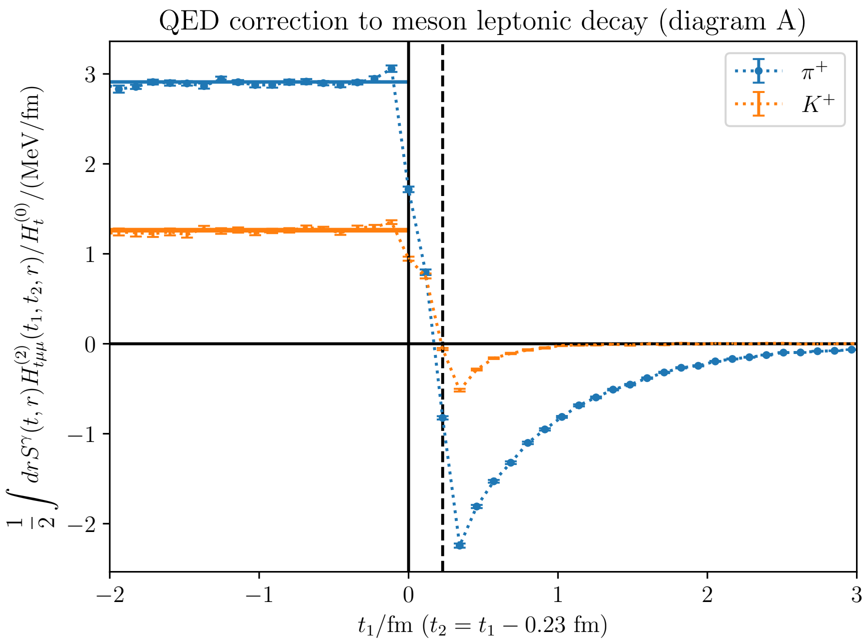

- Horizontal band represent the corresponding value from the mass shift calculation.

$$H^{(2)}_{t\mu\mu}(t_1, t_2, r)/H^{(0)}_t \approx H^{(s)}_{\mu\mu}(t_1 - t_2, r) \qquad (t_1, t_2 \ll 0) \tag{66}$$

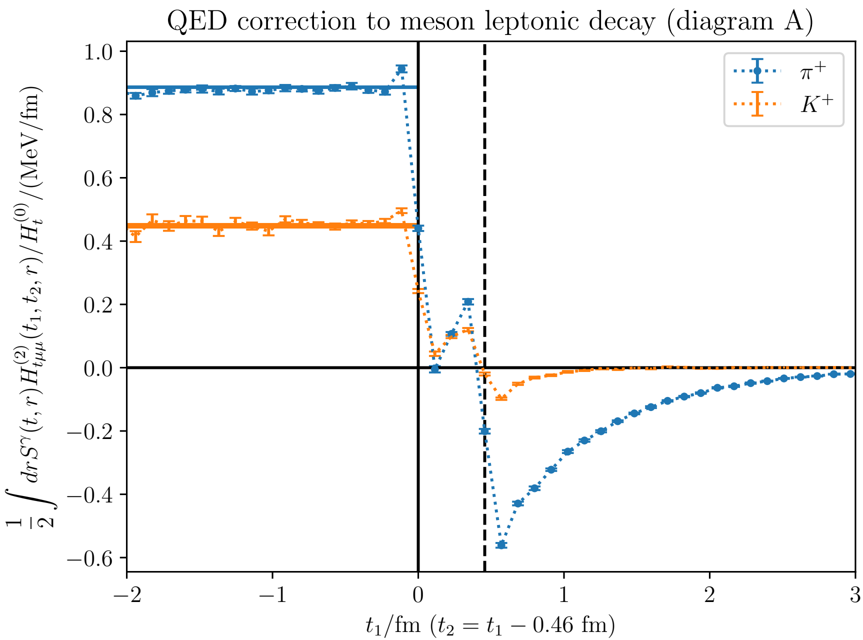

- Horizontal band represent the corresponding value from the mass shift calculation.

$$H^{(2)}_{t\mu\mu}(t_1, t_2, r)/H^{(0)}_t \approx H^{(s)}_{\mu\mu}(t_1 - t_2, r) \qquad (t_1, t_2 \ll 0) \qquad (67)$$

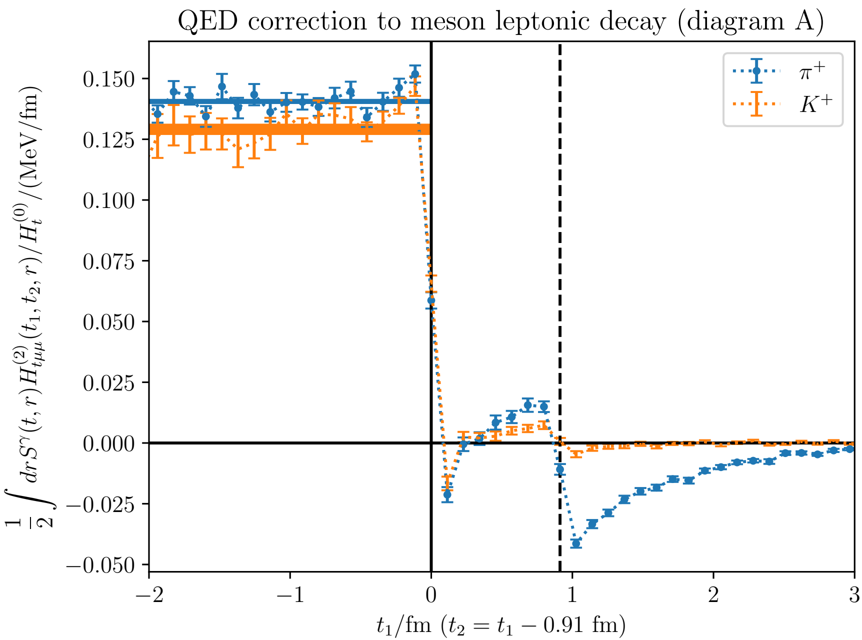

- Horizontal band represent the corresponding value from the mass shift calculation.

$$H^{(2)}_{t\mu\mu}(t_1,t_2,r)/H^{(0)}_t \approx H^{(s)}_{\mu\mu}(t_1-t_2,r) \qquad (t_1,t_2 \ll 0) \tag{68}$$

Summary

- Infinite volume reconstruction method (IVR) can be used to control the finite volume effects in many QED + QCD lattice calculations.
- We calculate the QED corrections to meson masses.
- We studied the operator renormalization via operator product expansion (OPE).
- We calculate the matrix elements related to QED corrections to meson leptonic decay.

Thank You!